ARTICLE

Large-Area Roll-to-Roll and Roll-to-Plate Nanoimprint Lithography: A Step toward High-Throughput Application of Continuous Nanoimprinting

Se Hyun Ahn[†] and L. Jay Guo[‡,*]

[†]Department of Mechanical Engineering and [‡]Department of Electrical Engineering and Computer Science, University of Michigan, Ann Arbor, Michigan 48109

ABSTRACT A continuous roll-to-roll nanoimprint lithography (R2RNIL) technique can provide a solution for high-speed large-area nanoscale patterning with greatly improved throughput; furthermore, it can overcome the challenges faced by conventional NIL in maintaining pressure uniformity and successful demolding in large-area imprinting. In this work, we demonstrate large-area (4 in. wide) continuous imprinting of nanogratings by using a newly developed apparatus capable of roll-to-roll imprinting (R2RNIL) on flexible web and roll-to-plate imprinting (R2PNIL) on rigid substrate. The 300 nm line width grating patterns are continuously transferred on either glass substrate (roll-to-plate mode) or flexible plastic substrate (roll-to-roll mode) with greatly enhanced throughput. In addition, the film thickness after the imprinting process, which is critical in optical applications, as a function of several imprinting parameters such as roller pressure and speed, is thoroughly investigated, and an analytical model has been developed to predict the residual layer thickness in dynamic R2RNIL process.

KEYWORDS: nanoimprint lithography · patterning · roll-to-roll · roll-to-plate · flexible substrate · residual layer

*Address correspondence to guo@eecs.umich.edu.

Received for review April 9, 2009 and accepted June 22, 2009.

Published online July 2, 2009.
10.1021/nn9003633 CCC: $40.75

© 2009 American Chemical Society

Among many nonconventional nanopatterning techniques that have been developed in the past decade,[1] nanoimprint lithography (NIL) clearly stands out as a promising technology for high-throughput and high-resolution nanoscale patterning,[2,3] which can achieve resolutions beyond the limitations set by light diffraction or beam scattering that are encountered in other traditional techniques. The development in this area has enjoyed great momentum in the past decade, and numerous applications such as in Si electronics,[4,5] organic electronic and photonics,[6,7] magnetics,[8,9] and biology[10−13] have been exploited by many researchers. On the other hand, the current process and throughput in NIL (∼few min or longer per wafer) is still far from meeting the demands of many practical applications, especially in flat panel display, photonics, biotechnology, and organic optoelectronics. It is very attractive to develop a nanoimprint-based patterning technique that can be applied in a continuous roll-to-roll process to drastically increase the patterning speed. Furthermore, it can overcome the challenges faced by conventional NIL in maintaining pressure uniformity and successful demolding in large-area printing. Toward that end, Tan *et al.* have used a solid rod to apply pressure to a piece of Si mold in a thermal nanoimprint process.[14] Lee *et al.* proposed a bilayer transfer process from a "rigiflex" mold to a Si wafer and demonstrated continuous thermal nanoimprinting process.[15] In our previous work,[16,17] we presented fabrication of metal wire-grid polarizers done by continuous roll-to-roll imprinting of nanoscale structures (70 and 300 nm line width gratings) on a narrow flexible plastic substrate (10 mm width) using a flexible fluoropolymer mold and a fast thermal curable PDMS[18] and a liquid UV-curable epoxysilicone resist.[19] On the other hand, truly large area continuous imprinting is yet to be demonstrated. Also, in many applications, such as flat panel displays, rigid substrates such as glass plate are preferred over plastic substrates. In addition to the pattern quality and large-area printability, the film thickness after imprinting, which is commonly referred in NIL as the residual layer thickness (RLT) of the imprinted pattern, is an important factor, especially for subsequent etching process and for the patterned film to be used in optical applications. In this respect, the RLT in terms of initial resist thickness[20] and applied pressure[21] in conventional imprinting process have been studied. The filling of viscoelastic thermoplastic resist material into the mold cavity in a hot embossing process has been investigated,[22−25] and its dependency on polymer properties[26] and cavity geometry[27]

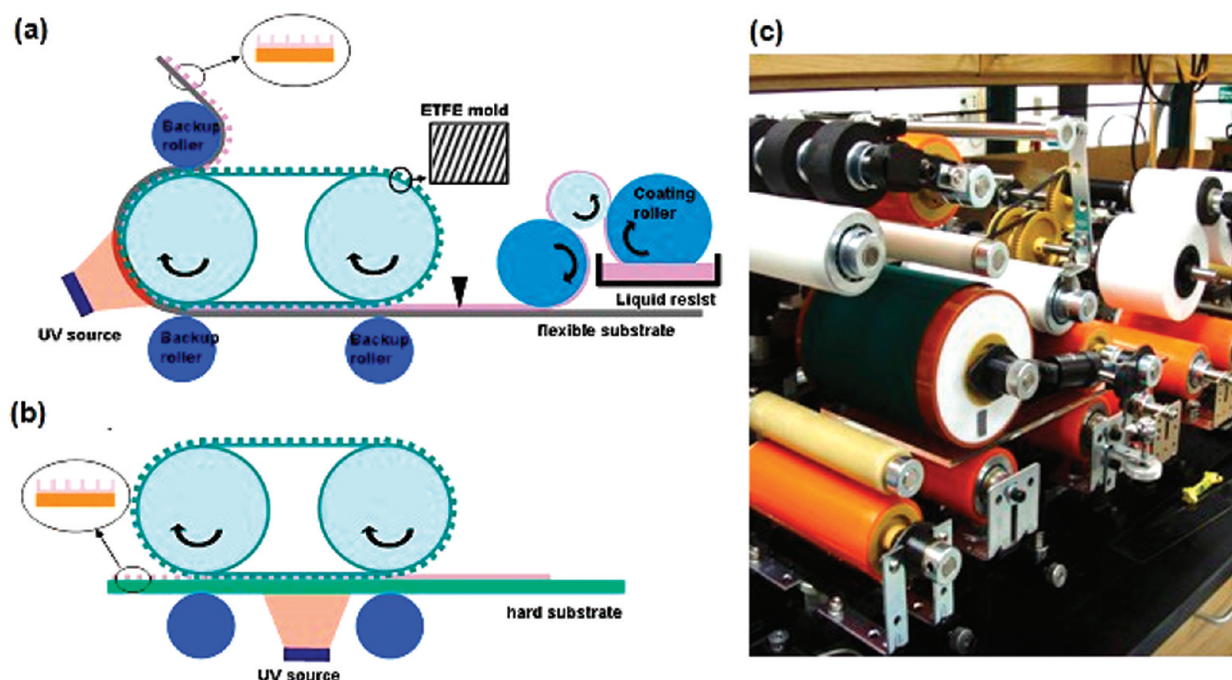

Figure 1. Schematics of (a) R2RNIL and (b) R2PNIL process. (c) Photograph of 6 in.-capable R2R/R2PNIL apparatus.

also have been exploited. In addition, the mold filling mechanism in a continuous imprinting process using flexible mold has been explored.[28] However, the model assumed that the squeezing action of two parallel plates is not very realistic in a dynamic roll-to-roll process. Apart from nanopatterning, flow property based on hydrodynamics and contact mechanics also has been studied by many researchers. Squeezing flow properties between two plates,[29] hard sphere to hard plane contact,[30] hard cylinder to elastic body contact,[31] and elastic sphere and hard plate contact[32] have been investigated.

In this work, we demonstrate large-area (4 in. wide) continuous imprinting of nanoscale structures by using a newly developed 6 in.-capable roll-to-plate (R2PNIL)/roll-to-roll (R2RNIL) apparatus, which can be potentially applied to many practical applications. The 300 nm line width grating patterns are imprinted continuously on either rigid glass substrate (R2PNIL mode) or flexible plastic substrate (R2RNIL mode) with greatly enhanced productivity. In addition, the residual layer thickness, which is critical in optical applications, as a function of several imprinting parameters such as the roller pressure and roller speed, has been thoroughly investigated. An analytical model was developed to predict the RLT, and the results are consistent with the experimental values.

Figure 1 shows the overall configuration of a continuous (a) R2RNIL and (b) R2PNIL nanomanufacturing process, which consists of two processing steps: (1) the coating process and (2) the imprinting-curing process. First, liquid phase UV-curable resist material is continuously coated on either flexible PET in R2RNIL or glass substrate in R2PNIL by a three-step roller coating system. The coating system is synchronized with the main imprinting roller to guarantee uniform coating thickness regardless of web speed. In our system, dual imprint rollers and a tensioned belt supported by the two rollers are used to allow large curing area and to maintain constant pressure during the curing process for fast patterning speed. The pressure between the imprint roller and the back-up roller is controlled by a clamping device and a force sensor. In this study, a flexible fluoropolymer, ethylene tetrafluoroethylene (ETFE), is used as a mold material. ETFE mold can be easily replicated from an original Si mold by a thermal NIL process at 220 °C. Moreover, the exceptional antisticking property of ETFE (surface energy of 15.6 dyn/cm, *cf.* PDMS ~19.6 dyn/cm) makes it easy to demold after imprinting without any mold surface treatment. In our experiment, several pieces of ETFE molds of proper size were replicated, wrapped, and fixed onto a 6 in. wide tensioned belt. For R2RNIL (Figure 1a) process, the resist material is imprinted by the dual rollers and the tensioned belt and then cured by a high-power UV source (Omnicure1000, EXPO) under the web tension at the second roller. On the other hand, in the R2PNIL (Figure 1b) process, UV curing of the imprinted resist material takes place between the two rollers under the pressure provided by the belt tension. Even though the normal component of the belt tension is smaller than that of the roller pressure, it is sufficient to maintain the resist film thickness after passing through the first roller. Through this process, nanograting patterns are continuously created on either PET or glass substrate as the ETFE mold continuously detaches from the imprinted resist on the substrate.

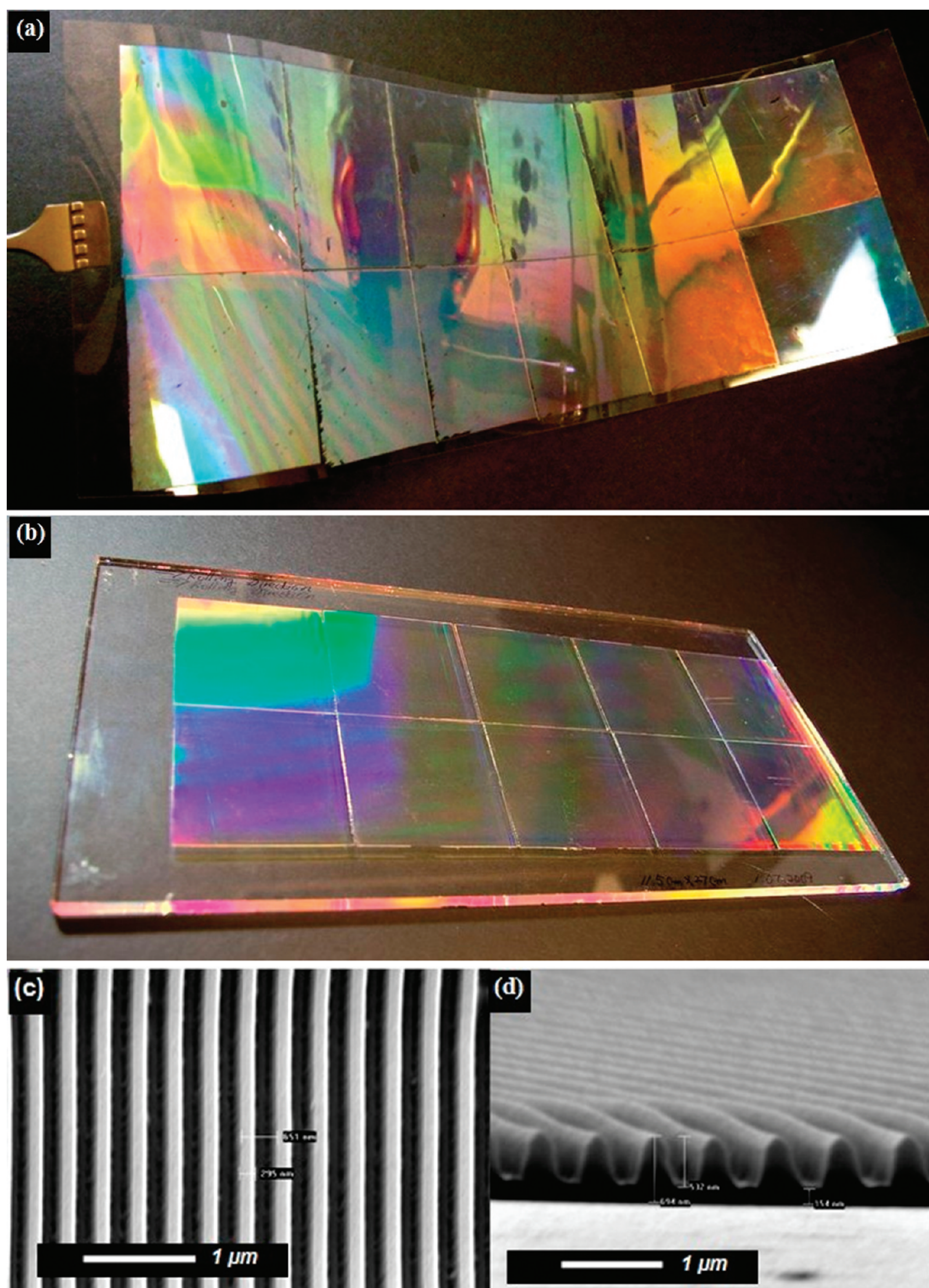

Figure 2. (a) A 4 in. wide, 12 in. long 700 nm period epoxysilicone pattern on flexible PET substrate by R2RNIL process and (b) a 4 in. wide, 10.5 in. long 700 nm period grating pattern on glass substrate. (c,d) SEM images of the patterned grating structure.

For a fast roll-to-roll process, we used a UV-curable low viscosity liquid epoxysilicone[19] as the imprint resist material. Different from the acrylate-based resists often used in the UV-assisted NIL process such as step-and flash imprint lithography (S-FIL),[33] epoxysilicone is cured *via* a cationic curing mechanism, thereby free from the oxygen inhibition issue when exposed in air. Thus no special vacuum environment is required, which is convenient for the roll-to-roll process. Furthermore, its very low shrinkage after curing (only a fraction of the

acrylate system) allows a faithful pattern replication. Owing to its low viscosity, the resist precursor can be imprinted at low pressures and cured within a second by focused UV light. The low pressure and the room temperature imprinting characteristics are advantageous for R2RNIL.

Figure 2a represents large-area (4 in. × 12 in.) nanograting patterns produced on a flexible PET plastic substrate by the R2RNIL process. Figure 2b shows the imprinted nanograting patterns on glass substrate by R2PNIL. The strong light diffraction from the 700 nm periodic grating structures can be clearly observed. As described earlier, several pieces of ETFE molds were attached to the tensioned belt, and the separation between them produces the seams that can be seen between the square-shape patterned areas. SEM images (Figure 2c,d) show that 300 nm line width and 600 nm height gratings are faithfully replicated onto the substrate. The light intensity used for UV curing is 110.8 mW/cm^2 in the central part. The fast curing of the epoxysilicone resist results in a web speed of 1 m/min, a 20-fold increase in imprinting speed as compared with that reported in ref 15. A requirement for achieving such a large-area nanopattern is that the resist material needs to have low adhesion to the mold and high adhesion to the substrate. For R2PNIL, we found that the epoxysilicone resist has relatively lower adhesion to the bare glass substrate, and so it tends to peel off from the substrate during the demolding process despite the low surface energy of the ETFE mold. To overcome this problem, the glass substrate is pretreated by oxygen plasma followed by the thermal deposition of an adhesion promoter (Silquest A187, GE Advance Materials).

In some optical applications, such as metal wire-grid polarizers and solar cells, the overall film thickness or the RLT of imprinted structure is very important due to light absorption or film birefringence. Moreover, most semiconductor applications prefer thinner RLT to minimize the impact on the pattern profile during the residual layer removal by the following plasma etching process. We will compare several analytical models to predict the RLT in a typical R2RNIL process.

Figure 3a depicts a process where the liquid resist is squeezed by two planar plates. In the solid plane squeeze model, the time (t) to reach the final film thickness (h_f) can be expressed as follows.[24]

$$t = \frac{\mu a^2}{2P}\left(\frac{1}{h_f^2} - \frac{1}{h_0^2}\right) = \frac{\mu a^3 L}{2F}\left(\frac{1}{h_f^2} - \frac{1}{h_0^2}\right)$$

where μ is the dynamic viscosity, h_0 the initial film thickness, L the width of the panel, F the force applied to the plates, and a the contacting length where resist gets squeezed by rollers (Figure 3a). From this equation, we can get the final RLT in terms of the applied force (F) and the web speed (V).

$$h_f = \left(\frac{2F}{\mu a^2 LV} + \frac{1}{h_0^2}\right)^{-1/2} \quad (1)$$

However, in practical roll-to-roll imprinting (R2RNIL), rather than two parallel plates, the resist is pressed by two cylindrical rollers that are wrapped with elastic cushion layers. In this case, the pressure distribution from the rollers is given by Hertz contact solution[34] as (elastic roller contact model, Figure 3b)

$$P = \frac{8F}{\pi a^2 L}\left(\left(\frac{a}{2}\right)^2 - x^2\right)^{1/2} \quad (2)$$

where F is the applied force.

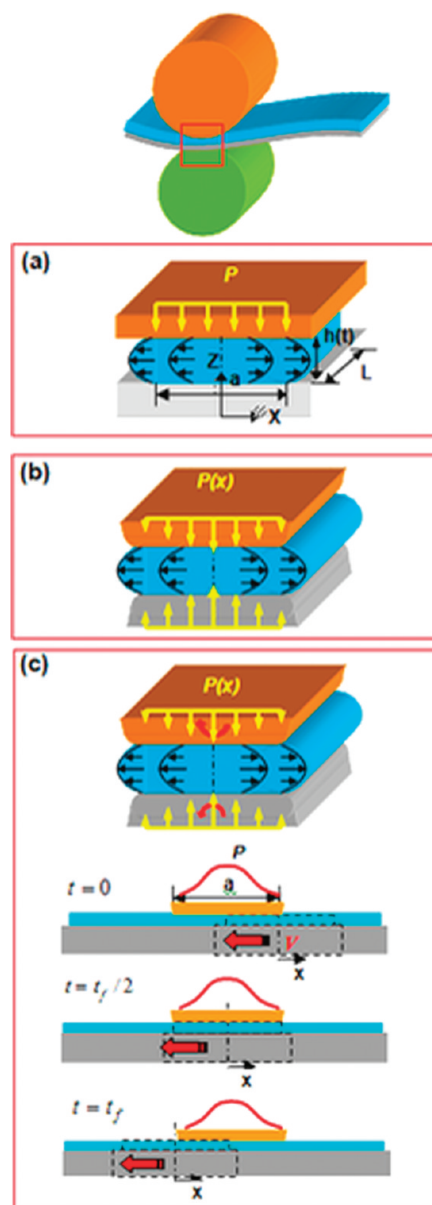

Figure 3. Schematic diagram of the liquid resist being squeezed by the contact rollers in (a) the solid plane squeeze model, (b) the elastic roller contact model, and (c) the dynamic elastic roller contact model.

By combining eq 2 with the Navier–Stokes equation, the final RLT at the center of contacted region from the elastic roller contact model becomes

$$h_f = \left(\frac{8F}{\pi\mu a^2 LV} + \frac{1}{h_0^2}\right)^{-1/2} \quad (3)$$

For more realistic modeling of the dynamic roll-to-roll imprinting where the liquid resist is squeezed between two rotating elastic rollers, we can consider time-dependent parabolic pressure distribution or the dynamic elastic roller contact model as shown in Figure 3c. In this model, every small element in the liquid resist experiences a pressure distribution as a function of time, t, as the roller moves. That is

$$P(t) = \frac{8F}{\pi a^2 L}\left(\left(\frac{a}{2}\right)^2 - \left(-\frac{a}{2} + V\cdot t\right)^2\right)^{1/2} \quad (4)$$

By equating it with the Navier–Stokes equation, the final RLT in the dynamic elastic roller contact model yields a simple expression

$$\therefore h_f = \left(\frac{F}{\mu a^2 LV} + \frac{1}{h_0^2}\right)^{-1/2} \quad (5)$$

To evaluate the three models and to compare with the experimental data, several assumptions will be made. First, in the modeling, we assume 2-D symmetric squeezed flow in z- and x-directions since the sample width, L, is much larger than contacting length, a. Second, the initial resist thickness (h_0) is set to 50 μm, which is close to the actual measurement data in our coating system. This assumption is reasonable because the dependence of RLT on the initial film thickness is negligibly small for the force range (50 to 300 N) used in our experiment. In addition, the accumulation of resist material (*i.e.*, increase of h_0) by back-squeezing as a roller moves also has negligible effect on the final RLT. For large h_0, the second term $1/h_0^2$ in each model in eqs 1, 3, and 5 is negligibly smaller than the first term in the force range used in our experiment. Third, for simple analysis, the contacting length between a roller and backing plate, a, is assumed to be a constant value,

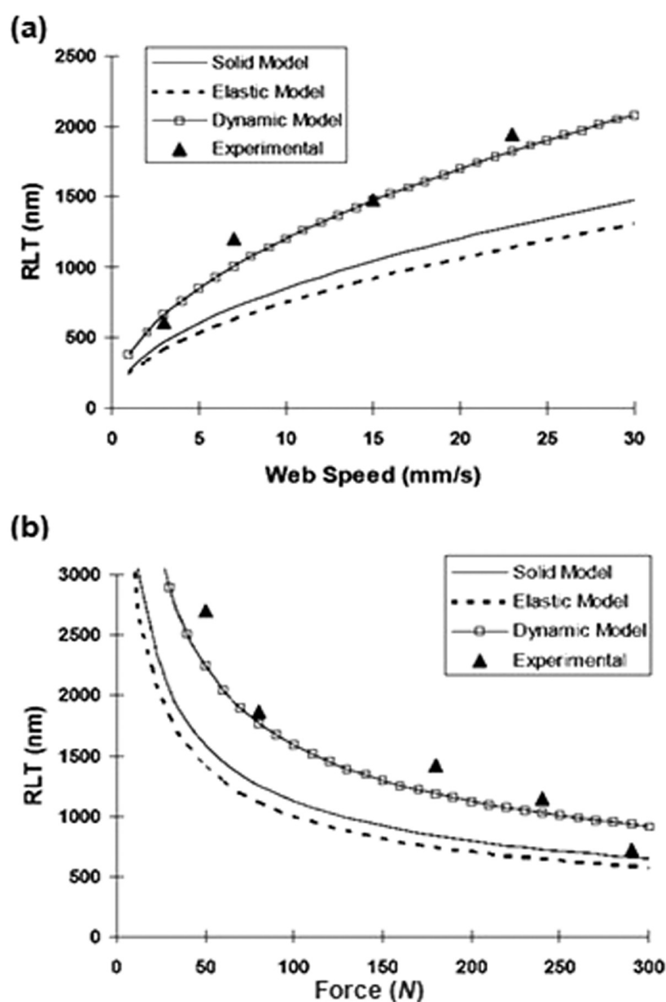

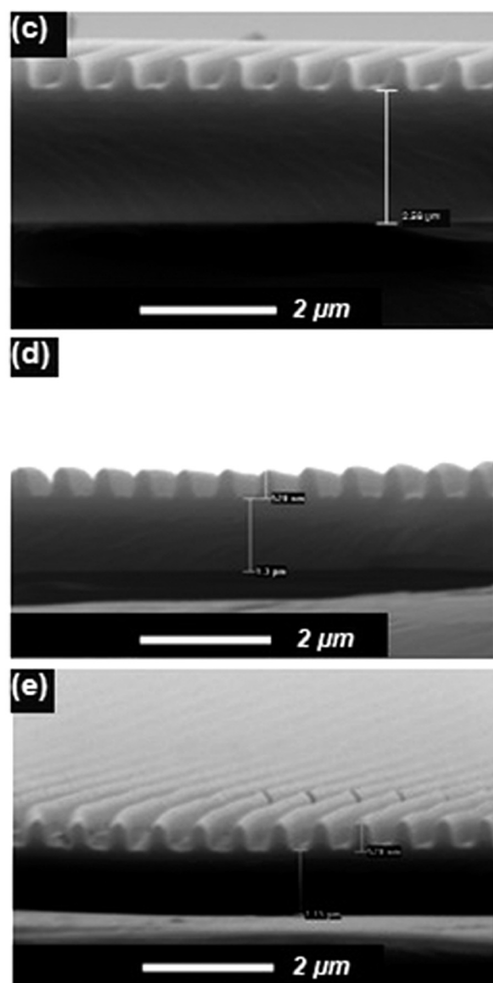

Figure 4. Comparison of three models (solid/elastic/dynamic model) for R2PNIL and experimental data (average value of three-time measurement). (a) RLT as a function of web speed with keeping maximum rolling force, 220 N. (b) RLT as a function of maximum rolling force with keeping web speed, 7.94 mm/s. SEM images of (b,c) 2.58 μm RLT for 50 N force, (d) 1.30 μm RLT for 180 N force, and (e) 1.15 μm RLT for 240 N force.

6.5 mm, which is the average measured value corresponding to the force range used in our experiment. Here, a is measured by the pressure sensing film (Tekscan, Inc.) under stationary condition. Although a is the function of applied rolling force, its deviation ($\pm$0.3 mm) in the force range of 50 to 300 N is small enough to be neglected. Finally, in each model, we consider 3% volumetric shrinkage of epoxysilicone resist after UV curing[19] to compare it with the experimental RLT data measured after cross-linking by UV curing. The dynamic viscosity (μ) of epoxysilicone resist is 0.032 Pa · s and sample width, L, is 25 mm.

Figure 4 shows RLT in each model (the solid plane squeeze, the elastic roller contact, and the dynamic elastic roller contact model) and the experimental data as a function of web speed (a) and applied rolling force (b). As shown in Figure 4a, RLT gets thicker as web speed increases because the pressure engaging time gets shorter. Figure 4b shows the expected result that the RLT decreases with increasing rolling force. In both graphs, all three models have similar trends but the dynamic elastic roller contact model has an almost perfect match to the experimental data, while the other two static models underestimate the RLTs. This implies that in the dynamic R2RNIL process it is important to consider the time-dependent force gradient in predicting the final residual layer thickness. Figure 4c−e shows RLT 700 nm period grating pattern in terms of applied roller force of 50, 180, and 240 N, respectively.

CONCLUSIONS

We have demonstrated large-area (4 in. wide) imprinting of 300 nm line width grating structures on either hard or flexible substrate by developing a new apparatus capable of both R2RNIL and R2PNIL processes with greatly enhanced throughput. In addition, we developed a more accurate model by taking into account the time-dependent pressure distribution for predicting the residual layer thickness as a function of the web speed and the rolling force in a dynamic R2RNIL process.

EXPERIMENTAL SECTION

Fabrication of ETFE Mold: A 200 μm thick ETFE film (SAINT-GOBAIN) was sandwiched between a Si mold containing grating structures and a Si substrate and pressed by a pressure machine with a temperature controller. A temperature of 220 °C and an imprint pressure of 2 MPa were used. After 5 min hot embossing, the sample was cooled to ambient temperature while keeping the pressure at 2 MPa. Then, the ETFE film was released from the Si mold by peeling manually.

Surface Treatment of Glass Substrate: To improve the adhesion of the glass substrate with the epoxysilicone resist, the glass substrate was pretreated by oxygen plasma (100 W, 250 mTorr, 10 min) followed by thermal deposition of adhesion promoter, Silquest187 (GE Advance Materials, 140 °C, 15 min).

R2R/R2P NIL: Several pieces of flexible ETFE molds were attached on a nitrile rubber-coated nylon fabric belt that is wrapped around two PTFE rollers. Liquid phase epoxysilicone resist material was continuously coated on the substrate in the coating module and cured by UV exposure (7.2 W/cm^2, EXFO Inc.), while roller pressure is applied. Web speed (1.3−23.5 mm/s) was controlled by an AC motor controller. Rolling force is measured in real-time by flexible force sensor (Tekscan, Inc.) and adjusted by a clamping device. Mold−substrate separation takes place continuously as the web moves forward.

Acknowledgment. The authors gratefully acknowledge the financial support NSF Grant No. CMII 0700718.

REFERENCES AND NOTES

1. Rogers, J. A.; Lee, H. H. *Unconventional Nanopatterning Techniques and Applications*; John Wiley & Sons: New Jersey, 2009.
2. Chou, S. Y.; Krauss, P. R.; Renstrom, P. J. Imprint of Sub-25 nm vias and Trenches in Polymers. *Appl. Phys. Lett.* **1995**, *67*, 3114–3116.
3. Chou, S. Y.; Krauss, P. R.; Renstrom, P. J. Imprint Lithography with 25-Nanometer Resolution. *Science* **1996**, *272*, 85–87.
4. Guo, L. J. Nanoimprint Lithography: Methods and Material Requirements. *Adv. Mater.* **2007**, *19*, 495–513.
5. Zhang, W.; Chou, S. Y. Fabrication of 60-nm Transistors on 4-in. Wafer Using Nanoimprint at All Lithography Levels. *Appl. Phys. Lett.* **2003**, *83*, 1632–1634.
6. Pisignano, D.; Persano, L.; Raganato, M. F.; Visconti, P.; Cingolani, R.; Barbarella, G.; Favaretto, L.; Gigli, G. Room-Temperature Nanoimprint Lithography of Non-thermoplastic Organic Films. *Adv. Mater.* **2004**, *16*, 525–529.
7. Kim, M.-S.; Kim, J.-S.; Cho, J.; Stein, M.; Guo, L. J.; Kim, J. Flexible Conjugated Polymer Photovoltaic Cells with Controlled Heterojunctions Fabricated Using Nanoimprint Lithography. *Appl. Phys. Lett.* **2007**, *90*, 123113.
8. Wu, W.; Cui, B.; Sun, X.; Zhang, W.; Zhuang, L.; Kong, L.; Chou, S. Y. Large Area High Density Quantized Magnetic Disks Fabricated Using Nanoimprint Lithography. *J. Vac. Sci. Technol., B* **1998**, *16*, 3825–3829.
9. Martin, J. I.; Nogues, J.; Liu, K.; Vicent, J. L.; Schuller, I. K. Ordered Magnetic Nanostructures: Fabrication and Properties. *J. Magn. Magn. Mater.* **2003**, *256*, 449–501.
10. Cao, H.; Yu, Z. N.; Wang, J.; Tegenfeldt, J. O.; Austin, R. H.; Chen, E.; Wu, W.; Chou, S. Y. Fabrication of 10 nm Enclosed Nanofluidic Channels. *Appl. Phys. Lett.* **2002**, *81*, 174–176.
11. Guo, L. J.; Cheng, X.; Chou, C. F. Fabrication of Size-Controllable Nanofluidic Channels by Nanoimprinting and Its Application for DNA Stretching. *Nano Lett.* **2004**, *4*, 69.
12. Falconnet, D.; Pasqui, D.; Park, S.; Eckert, R.; Schift, H.; Gobrecht, J.; Barbucci, R.; Textor, M. A Novel Approach to Produce Protein Nanopatterns by Combining Nanoimprint Lithography and Molecular Self-Assembly. *Nano Lett.* **2004**, *4*, 1909–1914.
13. Hoff, J. D.; Cheng, L. J.; Meyhofer, E.; Guo, L. J.; Hunt, A. J. Nanoscale Protein Patterning by Imprint Lithography. *Nano Lett.* **2004**, *4*, 853–857.
14. Tan, H.; Gilbertson, A.; Chou, S. Y. Roller Nanoimprint Lithography. *J. Vac. Sci. Technol., B* **1998**, *16*, 3926–3928.
15. Seo, S.-M.; Kim, T.-I.; Lee, H. H. Simple Fabrication of Nanostructure by Continuous Rigiflex Imprinting. *Microelectron. Eng.* **2007**, *84*, 567–572.
16. Ahn, S. H.; Guo, L. J. High-Speed Roll-to-Roll Nanoimprint Lithography on Flexible Plastic Substrate. *Adv. Mater.* **2008**, *20*, 2044–2049.
17. Ahn, S. H.; Kim, J.-S.; Guo, L. J. Bilayer Metal Wire-Grid Polarizer Fabricated by Roll-to-Roll Nanoimprint Lithography on Flexible Plastic Substrate. *J. Vac. Sci. Technol., B* **2007**, *25*, 2388–2391.
18. Pina-Hernandez, C.; Kim, J.-S.; Guo, L. J.; Fu, P.-F. High Throughput and Etch Selective Nanoimprinting and

Stamping Based on Fast Thermal-Curable Polydimethysiloxanes. *Adv. Mater.* **2007**, *19*, 1222–1227.

19. Cheng, X.; Guo, L. J.; Fu, P.-F. Room-Temperature, Low-Pressure Nanoimprinting Based on Cationic Photopolymerization of Novel Epoxysilicone Monomers. *Adv. Mater.* **2005**, *17*, 1419–1424.
20. Lee, H.-J.; Ro, H. W.; Soles, C. L.; Jones, R. L.; Lin, E. K.; Wu, W.-L. Effect of Initial Resist Thickness on Residual Layer Thickness of Nanoimprinted Structures. *J. Vac. Sci. Technol., B* **2005**, *23*, 3023–3027.
21. Lee, H. Effect of Imprinting Pressure on Residual Layer Thickness in Ultraviolet Nanoimprint Lithography. *J. Vac. Sci. Technol., B* **2005**, *23*, 1102–1106.
22. Scheer, H.-C.; Schulz, H. A Contribution to the Flow Behaviour of Thin Polymer Films During Hot Embossing Lithography. *Microelectron. Eng.* **2001**, *56*, 311–332.
23. Young, W.-B. Analysis of the Nanoimprint Lithography with a Viscous Model. *Microelectron. Eng.* **2005**, *77*, 405–411.
24. Heydermana, L. J.; Schifta, H.; Davida, C.; Gobrechta, J.; Schweizerb, T. Flow Behaviour of Thin Polymer Films Used for Hot Embossing Lithography. *Microelectron. Eng.* **2000**, *54*, 229–245.
25. Hirai, Y.; Konishi, T.; Yoshikawa, T.; Yoshida, S. Simulation and Experimental Study of Polymer Deformation in Nanoimprint Lithography. *J. Vac. Sci. Technol., B* **2004**, *22*, 3288–3293.
26. Schulz, H.; Wissen, M.; Bogdanski, N.; Scheer, H.-C.; Mattes, K.; Friedrich, C. Impact of Molecular Weight of Polymers and Shear Rate Effects for Nanoimprint Lithography. *Microelectron. Eng.* **2006**, *83*, 259–280.
27. Rowland, H. D.; Sun, A. C.; Schunk, P. R.; King, W. P. Impact of Polymer Film Thickness and Cavity Size on Polymer Flow During Embossing: Toward Process Design Rules for Nanoimprint Lithography. *J. Micromech. Microeng.* **2005**, *15*, 2414–2425.
28. Seo, S.-M.; Kim, T.-I.; Lee, H. H. Simple Fabrication of Nanostructure by Continuous Rigiflex Imprinting. *Microelectron. Eng.* **2006**, *84*, 567–572.
29. Denn, M. M.; Marrucci, G. Squeeze Flow Between Finite Plates. *J. Non-Newtonian Fluid Mech.* **1999**, *87*, 175–178.
30. Pascovici, M. D.; Cicone, T. Squeeze-Film of Unconformal, Compliant and Layered Contacts. *Tribol. Int.* **2003**, *36*, 791–799.
31. Hao, S.; Keer, L. M. Rolling Contact between Rigid Cylinder and Semi-infinite Elastic Body with Sliding and Adhesion. *J. Tribol.* **2007**, *129*, 481–494.
32. Persson, B. N. J.; Mugele, F. Squeeze-Out and Wear: Fundamental Principles and Applications. *J. Phys.: Condens. Matter* **2004**, *16*, 295–355.
33. Colburn, M.; Johnson, S. C.; Stewart, M. D.; Damle, S.; Bailey, T. C.; Choi, B.; Wedlake, M.; Michaelson, T. B.; Sreenivasan, S. V.; Ekerdt, J. G.; *et al.* Step and Flash Imprint Lithography: A New Approach to High-Resolution Patterning. *Proc. SPIE* **1999**, *3676*, 379–389.
34. Johnson, K. L. *Contact Mechanics*; Cambridge University Press: Cambridge, 1987.